2021

Development of a DNA Biosensor Using CRISPR/dCas9 on a Graphene Oxide Surface for Detecting Antibiotic Resistance Genes

Wendy Cecil

DEVELOPMENT OF A DNA BIOSENSOR USING CRISPR/DCAS9 ON A GRAPHENE OXIDE SURFACE FOR DETECTING ANTIBIOTIC RESISTANCE GENES

A Capstone Experience/Thesis Project Presented in Partial Fulfillment

of the Requirements for the Degree Bachelor of Science

with Mahurin Honors College Graduate Distinction

at Western Kentucky University

By

Wendy M. Cecil

August 2021

*****

CE/T Committee:

Dr. Moon-Soo Kim, Chair

Dr. Ajay Srivastava

Dr. Blairanne Williams

ABSTRACT

Antibiotic resistance is a rapidly spreading global threat to human health. Previously in our lab, we developed a simple method for facile detection of antibiotic resistance genes (ARGs) in bacteria. This DNA detection system takes advantage of the CRISPR-Cas system (Clustered Regularly Interspaced Short Palindromic Repeat and CRISPR-Associated Protein). We designed CRISPR in complex with nuclease deactivated Cas9 (dCas9) on graphene oxide (GO) sheets conjugated with Cas9 antibodies. Single guide RNA (sgRNA) was customized to program dCas9 for target DNA binding. sgRNA was covalently labeled with fluorescein to provide fluorescence signal. Graphene oxide (GO) is utilized for its quenching properties in this fluorescence resonance energy transfer (FRET) based DNA detection system and is based on the fluorescence quenching mechanism of antibody-GO (Ab-GO) in the absence and presence of target DNA. Cas9 antibodies (Abs) are first chemically conjugated to the GO surface, and conjugation was confirmed by atomic force microscopy (AFM). Previously, we validated the approach by performing a sensitivity assay to detect dsDNA within the tetracycline (tetM) resistance gene. This study is an extension of our prior work, which aimed to improve dCas9 protein purification and perform a quenching efficiency assay to confirm the optimal Ab-GO concentration as 2 μg/mL.

I dedicate this thesis to my older and younger brothers, Robbie Cecil and Daniel Cecil, respectively. Thank you for giving me examples to look up to and for allowing me to be the example as well.

ACKNOWLEDGEMENTS

Thank you to the Gatton Academy for introducing me to WKU and giving me the opportunity to learn what research was for the first time in 2016. Thank you to Dr. Moon-Soo Kim and Dr. Cathleen Webb for supporting my educational and research journeys in science. Thank you to WKU for 5 years of fun, rigor, and friendship.

VITA

EDUCATION

Western Kentucky University, Bowling Green, KY — Aug. 2021
B.A. in Molecular Biotechnology, B.A. in Biochemistry
Mahurin Honors College Graduate
Honors CE/T: *Development of a DNA Biosensor Using CRISPR/dCas9 on a Graphene Oxide Surface for Detecting Antibiotic Resistance Genes*

The Gatton Academy of Mathematics and Science, Bowling Green, KY — May 2018

Bardstown High School, Bardstown, KY — June 2018

PROFESSIONAL EXPERIENCE

Department of Chemistry, WKU — Sept. 2016-
Undergraduate Researcher — Aug. 2021

AWARDS & HONORS

Cum Laude, WKU, Aug 2021
First Place Session Winner, Southeast Regional IDEA Conference, 2019
Gatton Academy & Craft Academy Graduates Research and Experiential Learning Award, WKU, 2019
International Research Experience for Students, NSF, 2018
First Place Session Winner, Kentucky Academy of Sciences Research Conference, 2018
Citation of Research Achievement, Posters-at-the-Capitol, 2018
Horatio Alger Association State Scholar, 2018
First Place Session Winner, WKU Research Conference, 2017
First Place Session Winner, Kentucky Academy of Sciences Research Conference, 2017
WKU Sisterhood Research Internship Grant, WKU, 2017

PROFESSIONAL MEMBERSHIPS

American Chemical Society (ACS)

INTERNATIONAL EXPERIENCE

Cloudbridge Nature Reserve, Rivas, Costa Rica — Jan. 2018
Study Abroad and Research Experience, Gatton Academy, WKU

Chung-Ang University, Seoul, South Korea — June 2018-
NSF International Research Experience for Students — Aug. 2018

PRESENTATIONS

Poster Presentation, "Novel dsDNA Biosensor Utilizing Zinc Finger Proteins on 2D Graphene Oxide Surface for Detecting Antibiotic Resistance Genes," WKU Virtual Student Research Conference, May 2020.

Poster Presentation, "Zinc finger proteins on graphene oxide surface for detecting antibiotic resistance genes," KY NSF EPSCoR Annual Super Collider Conference, Lexington, KY, February 2020.

Poster Presentation, "Novel application of 2D nanosheet and DNA binding proteins for detecting antibiotic resistance genes," Southeast Regional IDEA Conference, Louisville, KY, November 2019.

Poster Presentation, "Developing a double-stranded DNA biosensor using engineered zinc finger proteins linked to a β-lactamase for detecting antibiotic resistance genes," American Chemical Society, Orlando, FL, April 2019.

Poster Presentation, "Development of a Double-Stranded DNA Biosensor Using Engineered Zinc Finger Protein Pairs Linked to a Full β-lactamase for Detecting Antibiotic Resistance Genes," WKU Student Research Conference, March 2019.

Poster Presentation, "Cultivation of Peanuts in Oak Tree Saw Dust to Increase Resveratrol," Kentucky Academy of Science Annual Meeting, November 2018.

Oral Presentation, "A Study of Mercury in Bald Eagle Feathers and Quills," WKU Student Research Conference, March 2018.

Poster Presentation, "A Study of Mercury in Bald Eagle Feathers and Quills," Posters-at-the-Capitol, February 2018.

Oral Presentation, "A Study of Carbon Storage in a Costa Rican Cloud Forest," Research Showcase in Costa Rica, January 2018.

Oral Presentation, "A Study of Mercury in Bald Eagle Feathers and Quills," Kentucky Academy of Sciences, November 2017.

Oral Presentation, "A Study of Mercury in Bald Eagle Feathers," WKU Student Research Conference, March 2017.

CONTENTS

Abstract ii

Acknowledgements iv

Vita v

List of Figures ix

List of Tables x

Chapter I: Introduction 1

1. Antibiotic Resistance (ABR)……...1

2. Aims of Study……..2

3. CRISPR-Cas Systems……..2

4. Graphene Oxide and Fluorescence Resonance Energy Transfer…….4

5. CRISPR/dCas9 GO-FRET Based DNA Sensing…….5

Chapter II: Experimental……..……7

1. Protein Expression and Purification ……7

2. sgRNA Design…….8

2.1 sgRNA Template Synthesis……...9

2.2 Invitro Transcription (IVT) Reaction……...10

2.3 PCR Amplification of Target DNA…….11

2.4 Cas9 Cleavage Assay……...12

2.5 sgRNA Labeling……..12

3. Antibody-conjugated Graphene Oxide (Ab-GO) ……..……15

4. Ab-GO Quenching Efficiency Assay…….16

Chapter III: Results and Discussion……...18

1. Protein Purification……...…….18

2. sgRNA Template Synthesis……...……21

2.1 Cas9 Cleavage Assay Before sgRNA Labeling……...22

2.2 Cas9 Cleavage Assay After sgRNA Labeling…….23

3. Ab-GO Surface Morphologies……...25

4. Quenching Efficiency Assay……..27

Chapter IV: Conclusions 30

Bibliography 31

LIST OF FIGURES

Figure 1. CRISPR/Cas9 immune system…….……...…..…3

Figure 2. Crystal structures of Cas9 and dCas9……...……3

Figure3. Structure of graphene oxide.…….……..…4

Figure 4. Basic principle of FRET……...…5

Figure 5. Schematic diagram of CRISPR/dCas9 GO-FRET assay.…….6

Figure 6. Vector map of plasmid pMJ841……..……7

Figure 7: sgRNA design and template synthesis…….9

Figure 8. Target DNA amplicon design…….…11

Figure 9: "Label IT" nucleic acid labeling kits……13

Figure 10. Nickel column and TEV cleavage SDS-PAGE analysis.…….…....19

Figure 11. Ni-NTA resin and cation exchange chromatography SDS-PAGE analysis….21

Figure 12. sgRNA_2 DNA template synthesis.……..…...22

Figure 13. Cas9 cleavage assay before sgRNA labeling…….…..23

Figure 14. Cas9 cleavage assay after sgRNA labeling……..24

Figure 15. Bare GO AFM surface morphology ……26

Figure 16. GO activated with EDC: NHS AFM surface morphology……...…26

Figure 17. Ab-GO AFM surface morphology…….…..26

Figure 18. Quenching efficiency analysis.…….27

LIST OF TABLES

Table 1. Expected protein sizes.……...…...…..18

Table 2. base:dye labeling ratios for sgRNA_2.……24

CHAPTER I - INTRODUCTION

1. Antibiotic Resistance

Antibiotic resistant bacteria (ARB) are an expanding threat to global and human health, predicted to cause 10 million deaths annually by 2050.[1, 2] The cost of antibiotic resistant (AR) infections to the US health care system is $21 billion to $34 billion each year.[3] Environmental reservoirs of AR exist in clinical and agricultural settings due to the estimated millions of metric tons of antibiotic compounds released into the biosphere by humans in recent decades.[4] Resistant bacterial populations spread when antibiotics exert selective pressures that favor resistance. AR is spreading rapidly because multiple unrelated pathogens can acquire evolved antibiotic resistance genes (ARGs) through horizontal gene transfer.[2] Currently, no known method exists to eliminate antibiotic resistance, yet promising potential solutions for the AR crisis exist such as bacteriophage therapy.[3] Combating the spread of ARB could be facilitated by their detection, aiding in prevention and treatment, through the development of specific ARG diagnostic tests.[5] Simple, sensitive, and rapid DNA detection technologies are vital for applications in public health.[6-9] Polymerase chain reaction (PCR) is the most widely used method for nucleic acid amplification, yet it requires multiple primers and precise thermal cycling conditions, rendering it difficult to apply in non-laboratory and low-resource settings.[10, 11]

2. Aims of Study

The objective of this study is to develop a diagnostic biosensor for ARG detection. This work expands on a prior project in our lab and takes advantage of the CRISPR-Cas system (Clustered Regularly Interspaced Short Palindromic Repeat and CRISPR-Associated Protein) and graphene oxide (GO) for detecting sequences on the tetracycline resistant gene (tetM).

3. CRISPR-Cas Systems

The CRISPR and Cas proteins are adaptive immune systems of most archaea and bacterial cells against invasion from foreign nucleic acids. The CRISPR/Cas system utilizes antisense RNA as a memory signature from previous viral invasion. A CRISPR locus is made up of a CRISPR array of short direct repeats interspaced by short variable DNA sequences called spacers.[12] The mechanism of CRISPR/Cas begins with the acquisition of foreign fragments of invading viral or plasmid DNA, known as protospacers, into the CRISPR array. These spacers provide recognition sequences for targeted destruction of subsequent viral or plasmid DNA. The selection of protospacers depends in part on the specific recognition of protospacer adjacent motifs (PAMs) present within the viral genome. In many CRISPR/Cas systems, recognition of a short protospacer adjacent motif (PAM) in the target DNA is required prior to protospacer acquisition. Next, the CRISPR array undergoes the biogenesis step of transcription and maturation processes for precursor transcript (pre-crRNA) synthesis, which later matures into a CRISPR RNA (crRNA).[13] In the final interference step, the association of crRNA and Cas proteins form a CRISPR/Cas endonuclease for the specific targeting and cleavage of cognate viruses or plasmids DNA.[12, 13]

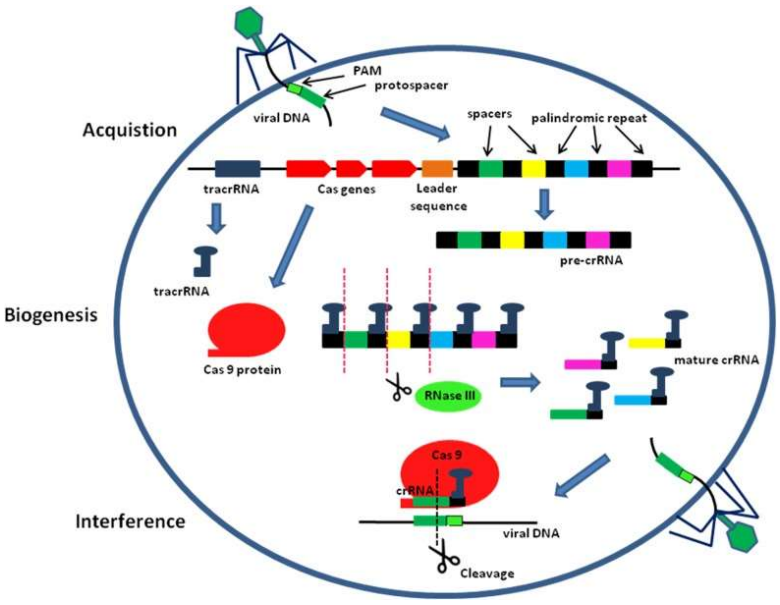

Figure 1: CRISPR/Cas9 immune system.[13]

The CRISPR/Cas system is a valuable programmable modular technology which may be employed for the rapid and early detection of antibiotic resistant bacteria or pathogens to aid therapeutic treatment.[14] Several unique CRISPR/Cas systems have been developed in recent years, showing promise for their use as rapid diagnostics with high sensitivity.[6, 10, 11, 15, 16]

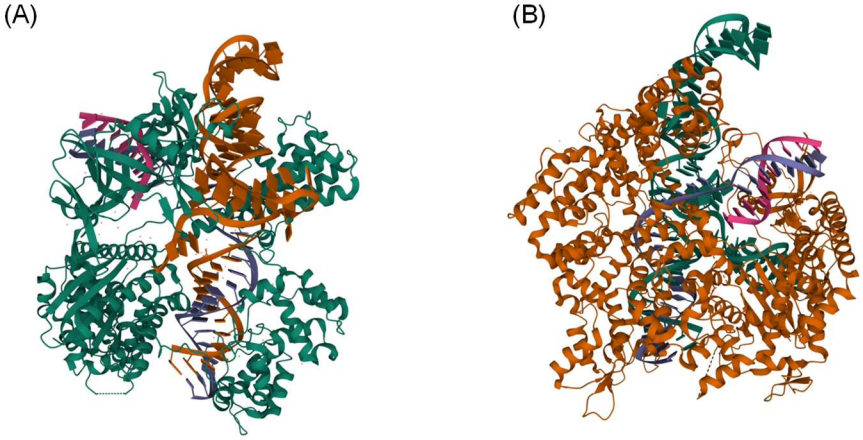

Figure 2: Crystal structures of Cas9 and dCas9. (A) PDB ID 5AXW Crystal structure of Staphylococcus aureus Cas9 in complex with sgRNA and target DNA (TTGGGT PAM).[17]

(B) PDB ID 6K57 Crystal structure of dCas9 in complex with sgRNA and DNA (CGA PAM).[18]

4. Graphene Oxide and Fluorescence Resonance Entergy Transfer (FRET)

GO is a two-dimensional carbon nanostructure that is one atom thick.[19-21] GO has unique physical properties such as large specific surface area, water solubility, electrical and optical characteristics, and biocompatibility.[20, 22] The surface of GO contains carbonyl and carboxylic groups at the edges, and hydroxyl and epoxy groups mainly at the basal plane, as seen in Figure 3.[20, 21] GO is known to non-covalently interact with biomolecules; GO adsorbs both nucleic acids and amino acids through π- π stacking or through hydrogen bonding and electrostatic interaction, respectively. Additionally, GO may be chemically modified for covalent conjugation to biomolecules.[23, 24]

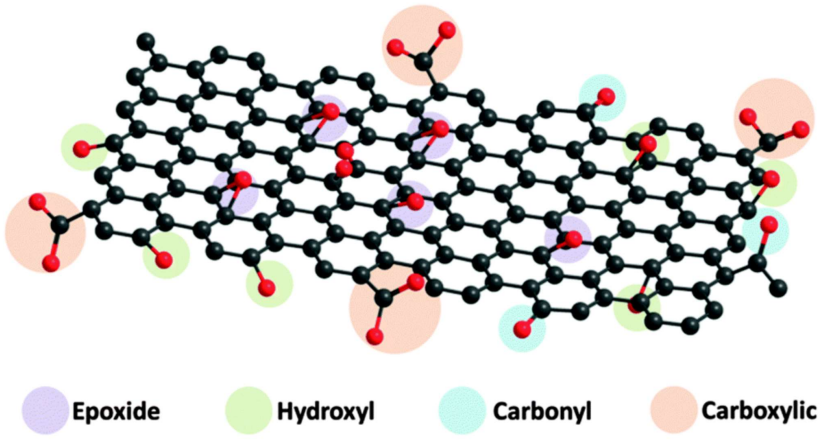

Figure 3: Structure of graphene oxide.[25]

GO has been used for applications in fluorescent sensing technology since it is a universal quencher for fluorescent molecules, making it ideal for fluorescence resonance energy transfer (FRET). FRET occurs between two photosensitive molecules, one of which donates and the other accepts energy. The donor fluorophore, initially in its electronically excited state, transfers energy to an acceptor chromophore as shown in

Figure 4.[26] An acceptor may emit or quench the energy, either of which may be favorable depending on the desired application of FRET. The FRET efficiency depends on the spectral overlap of the donor emission spectrum and the acceptor absorption spectrum, the distance between the donor and the acceptor (1–10 nm), and the relative orientation of the donor emission dipole moment and the acceptor absorption dipole moment.[26] For a traditional single FRET pair of fluorophores, the efficiency of FRET is inversely proportional to the sixth power of the distance between donor and acceptor, making FRET extremely sensitive to small changes in distance (r) between the donor and the acceptor.[26]

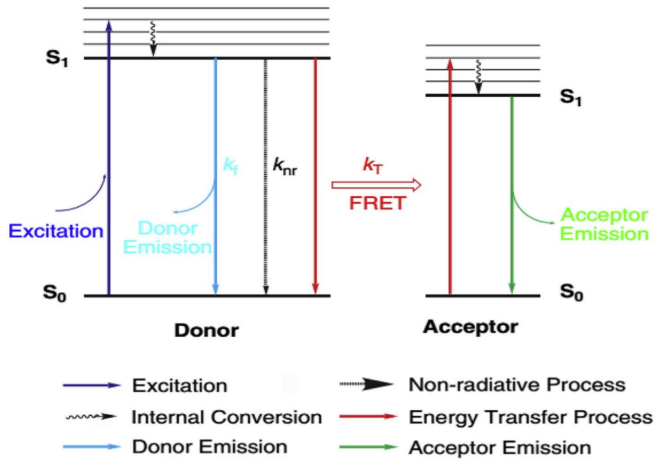

Figure 4: Basic principle of FRET.[26]

5. CRISPR/dCas9 GO-FRET Based DNA Sensing

GO is utilized for its quenching properties in this FRET based DNA detection system. First, CRISPR-Associated Protein 9 (Cas9) antibodies (Abs) are chemically conjugated to the GO surface. The Ab-GO is incubated with deactivated Cas9 (dCas9); consequently, dCas9 will bind to the antibodies on the GO surface. Fluorescein is a fluorophore covalently labeled to single guide RNA (sgRNA) to provide fluorescence

signal in the assay. The FRET based on/off fluorescent signal is directly influenced by the presence or absence of target DNA, respectively. Labeled sgRNA is incubated with the dCas9 immobilized on Ab-GO and will bind to dCas9, bringing the sgRNA in close proximity to GO. Thus, the labeled sgRNA signal will be quenched due to FRET in the absence of target DNA. The quenching capability of the Ab-GO sheet on labeled sgRNA relies on dCas9 immobilization to the Ab-GO surface and subsequent binding of sgRNA to dCas9. The sgRNA is complementary to the target and programs dCas9 to bind to the target DNA. Upon recognition of target DNA by dCas9, a conformational change will occur which will reduce the affinity of the dCas9/sgRNA_fluorescein/dsDNA complex from the Ab-GO surface. The dCas9/sgRNA_fluorescein/dsDNA complex will dissociate from Ab-GO, causing a physical separation of labeled sgRNA from Ab-GO, which does not allow FRET to occur anymore, thus restoring the fluorescent signal.

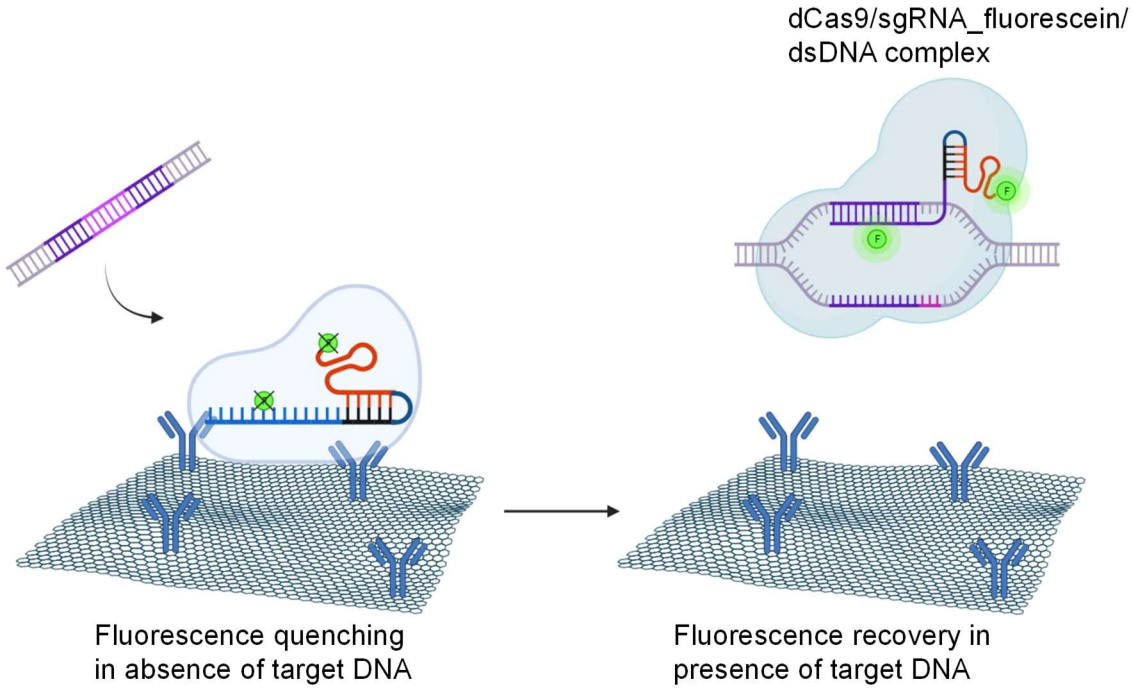

Figure 5: Schematic diagram of CRISPR/dCas9 GO-FRET assay (created with BioRender.com).

CHAPTER II - EXPERIMENTAL

1. Protein Expression and Purification

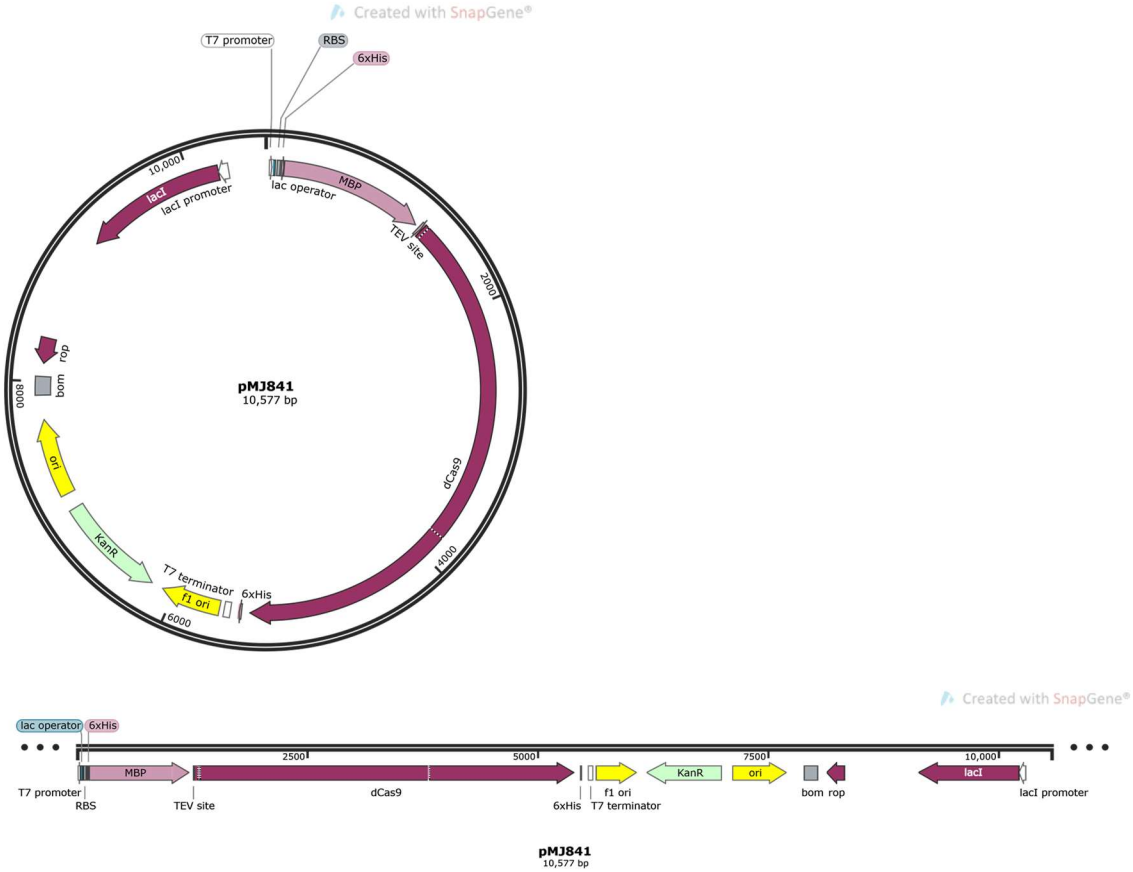

Figure 6: Vector map of plasmid pMJ841.

pMJ841 was a gift from Jennifer Doudna (Addgene plasmid # 39318; http://n2t.net/addgene:39318; RRID:Addgene 39318). The following protein purification protocol was adapted mainly from two references.[27, 28] The pMJ841 plasmid was transformed into Escherichia coli BL21 Rosetta 2 (DE3) (Invitrogen). Cells were grown at 37°C in terrific broth containing 25 µg/ mL kanamycin for 12-16 hours at 250 rpm, and then scaled up to 1 L. dCas9 expression was induced using 1 mM isopropyl 1-thio-β-D-

galactopyranoside (IPTG) at an OD600 of 0.6 for 16 hours at 16°C. Cells were harvested by centrifugation and resuspended in buffer A (20 mM Tris pH 8.0, 500 mM NaCl, 20 mM imidazole, 2 mM TCEP) with 1X final concentration protease inhibitor cocktail (Roche) and lysed by sonication. The soluble protein was obtained by centrifugation for 1 hour at 16,000g. The cell lysate was applied to a 1 mL HisTrap (GE LifeSciences) already equilibrated with buffer A and was washed with buffer A and subsequently with buffer containing 1 M NaCl and 250 mM NaCl. dCas9 was eluted using 20 mM Tris pH 8.0, 250 mM NaCl, 10% glycerol, 250 mM imidazole, 1 mM TECP. Eluate was adjusted to 1 mM DTT and 0.5 mM EDTA, and then dialyzed over night at 4°C against buffer B (25 mM HEPES pH 7.5, 1 mM TCEP, 10% glycerol) containing 150 mM KCl. Tobacca Etch Virus (TEV) protease was added and incubated at 30°C for 1 hour. The cleaved dCas9 protein was separated from the fusion tag using the HisPur™ Ni-NTA Resin (Thermo Scientific) Procedure for Purification of His-Tagged Proteins by Batch Method per the manufacturer's protocol or by chromatography on a 1 mL HiTrap SP FF (GE LifeSciences) column, in buffer B containing appropriate KCl concentrations for each step. Purified dCas9 aliquots in 25 mM HEPES pH 7.5, 150 mM KCl, 1 mM TCEP and 10% glycerol were stored on ice at 4°C. Protein concentration and purity were determined by Coomassie-stained polyacrylamide gel electrophoresis with sodium dodecyl sulfate (SDS−PAGE) and the Bradford assay using bovine serum albumin (BSA) standards.

2. sgRNA Design

The sgRNA candidate sequences for detecting the tetM gene were screened using the online Benchling CRISPR design tool (https://www.benchling.com/). Of the

generated 20-nt sgRNAs, five were selected based high specificity and efficiency score criteria in addition to target sequence adjacency to a 5' NGG protospacer adjacent motif (PAM) sequence. Four of the sgRNA designed were complementary to the non-template strand, and one was complementary to the template strand. Higher targeting efficiency is achieved when sgRNA binds to the non-template DNA strand, else CRISPR efficiency is repressed.

Forward PCR primers were designed to amplify DNA templates used for sgRNA synthesis. A forward primer is 56- to 58-nt and from 5' to 3' includes a T7 promoter sequence plus four extra bases, a transcription initiation site, the specific sgRNA target sequence, and the Guide-it Scaffold Template-annealing sequence. Forward primers were synthesized by IDT.

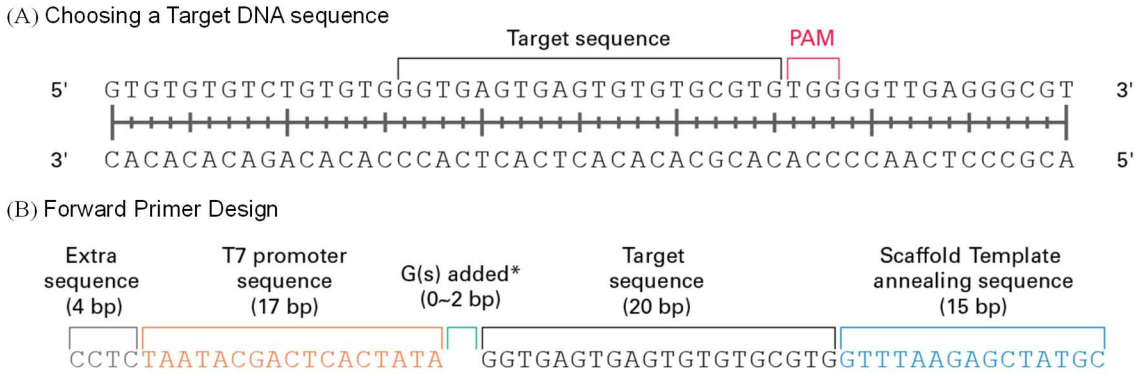

Figure 7: sgRNA design and template synthesis.

2.1 sgRNA Template Synthesis

DNA templates for sgRNA synthesis were amplified by PCR under the cycle conditions from the Guide-it sgRNA in Vitro Transcription system (Takara) manufacturer's protocol. In a 200 µL PCR tube, a 50 µL mixture was prepared containing 1 µL of the forward primer (10 µM) + 2 µL Guide-it Scaffold template + 25 µL

PrimeSTAR Max premix + 22 µL RNase Free water. After amplification of the template, 5 µL of the PCR product was analyzed on a 1.2% agarose gel with a 100-bp DNA ladder.

2.2 In Vitro Transcription (IVT) Reaction and Purification

The PCR product of sgRNA template synthesis was directly used for the In Vitro Transcription (IVT) Reaction without purification. In a 200 µL PCR tube, a 40 µL mixture was prepared containing 10 µL sgRNA PCR template + 14 µL Guide-It In Vitro Transcription buffer + 6 µL Guide-it T7 polymerase mix + 10 µL RNase free water. The mixture was briefly vortexed and spun down then placed in thermal cycler for 8 hours at 30°C and 4°C infinite hold. Following incubation, 4 µL of Recombinant DNase I (RNase-Free) was added to the 40 µL IVT reaction. The reaction (44 µL) was briefly vortexed and spun down then placed in a preheated thermal cycler for 15 minutes at 37°C and a 4°C infinite hold.

Transcribed sgRNA was purified using the Guide-it IVT RNA Clean-Up Kit (Takara). The reaction mixture was brought up to 100 µL with RNase free water, and everything was transferred to a 1.5 mL centrifuge tube. Then, 60 µL of IVT Binding Buffer + 130 µL of isopropanol were added and vortexed for 5 seconds after each addition. An IVT RNA Clean-Up Spin Column was placed in a collection tube and the sample was loaded onto the column for centrifugation at 11,000g for 30 seconds at room temperature. The flow through was discarded and the column was returned to the collection tube. 600 µL of IVT Wash Buffer was applied to the column and centrifuged at 11,000g for 30 seconds at room temperature. The flow through was discarded and the column was placed back in the collection tube. 250 µL of IVT Wash Buffer was applied and centrifuged at 11,000g for 2 min at room temperature. The flow through was

discarded and the column was placed into a new 1.5 mL micro centrifuge tube for elution. sgRNA was eluted with 22 µL of RNase free water added directly onto the silica membrane of the spin column and incubated for 1 minute at room temperature. The purified sgRNA was collected by centrifuging at 11,000g for 1 min at room. A nanodrop was used to determine sgRNA yield.

2.3 PCR Amplification of Target DNA

Purified sgRNA targets were screened for successful cleavage of their targets using the Guide-it sgRNA Screening Kit (Takara). Forward and reverse primers were designed to amplify the tetM regions targeted by the five sgRNAs. The optimal amplicon size for the Cas9 cleavage assay is 600–800 bp, with the sgRNA target sequence located asymmetrically within the amplicon and each cleavage fragment was at least 250 bp, and not greater than >100 bp size difference between the fragments after Cas9 cleavage. Successful cleavage would yield two fragments, with expected bands based on design criteria, distinguishable on an agarose gel. The PCR amplified target DNAs are also used as DNA targets for detection with CRISPR/dCas9 in the assay.

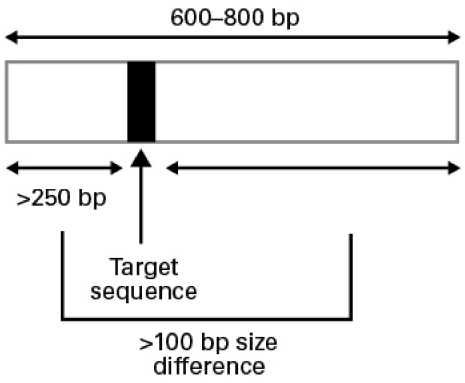

Figure 8: Target DNA amplicon design.

Target DNA was amplified by PCR according to the Guide-it Screening Systems (Takara) User Manual. In a 200 µL PCR tube, a 50 µL reaction was prepared using 25 µL

of 2X Terra PCR Direct Buffer (with Mg2+, dNTP) + 1.5 µL of forward primer (10 µM) + 1.5 µL of reverse primer (10 µM) + 1 µL of Terra PCR Direct Polymerase Mix (1.25 U/µl) + 20 µL of RNase Free Water + 1 µL of genomic DNA from Staphylococcus aureus subsp. aureus (ATCC 700699DQ). After incubation, 1 µL of 6X nucleic acid dye was added to 5 µL of the PCR product. On a 1.2% agarose gel, the PCR product and a 100 bp ladder were run at 100 V for 1 hour and 30 minutes.

2.4 Cleavage Assay

The Cas9 Cleavage Assay is used to confirm efficient cleavage of the DNA targets when sgRNAs are provided to CRISPR/Cas9. The cleavage assay was prepared according to the Guide-it sgRNA In Vitro Screening Kit. In a 200 µL PCR tube, the sgRNA/cas9 complex was prepared using target-specific sgRNA (350 ng) and 1 µL of Guide-it Recombinant Cas9 Nuclease (500 ng/ µL). The reaction was gently mixed well by pipetting and incubated using a thermal cycler at 37°C for 10 minutes. Then, the assay was performed in 15 µL reactions using 5 µL of PCR reaction solution (amplified target DNA) + 1 µL of 15X Cas9 Reaction Buffer + 1 µL of 15X BSA + 6.5 µL RNase free water + 1.5 µL Cas9/sgRNA mix. The reaction was gently mixed well by pipetting and incubated using a thermal cycler at 37°C for 1 hour and 80°C for 5 minutes. After incubation, 3 µL of nucleic acid 6X dye was added to the sample and then loaded on a 1.2 % agarose gel with a 100 bp ladder and run at 100 V for 1 hour and 30 minutes.

2.5 sgRNA Labeling and Purification

Fluorescein was covalently attached to the sgRNA using the *Label* IT Nucleic Acid Labeling Kit (Mirus). The *Label* IT chemical labeling reagents are composed of three regions as seen in Figure 9: the label (fluorophore or hapten) (green), the linker

(yellow) which facilitates electrostatic interactions with nucleic acids and the reactive alkylating group (blue) that covalently attaches the *Label* IT reagent to any reactive heteroatom within the nucleic acids. Attachment of the *Label* IT Reagents to nucleic acids does not alter the structure of the nucleic acid or affect downstream hybridization performance.

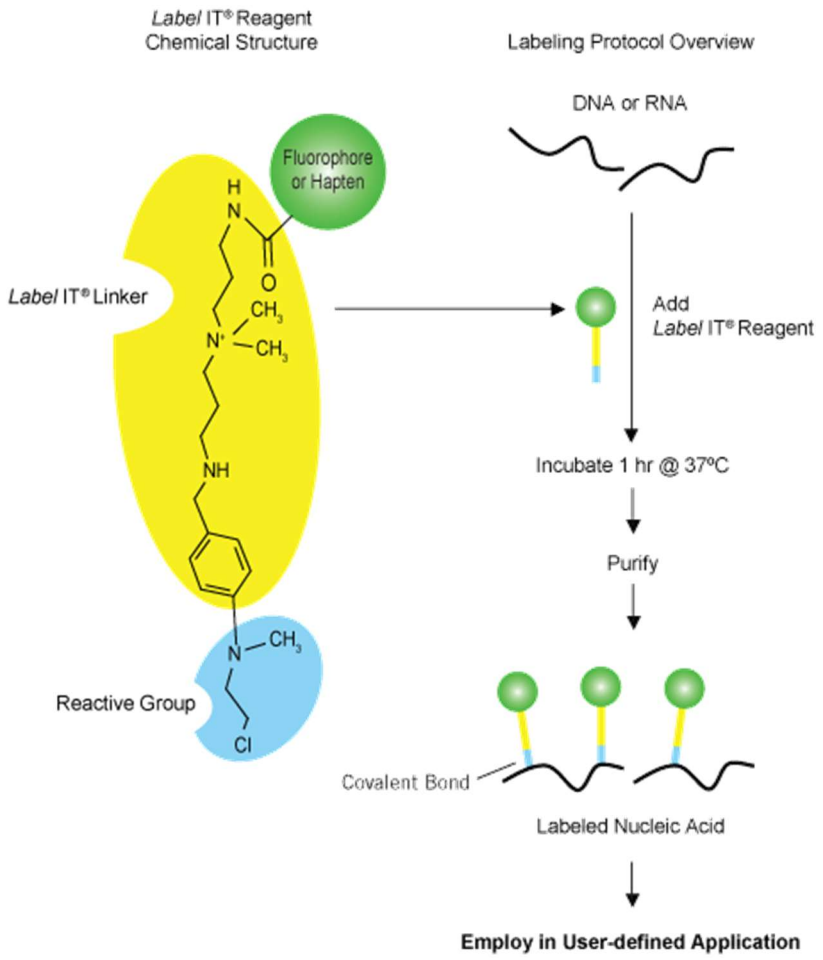

Figure 9: Label *IT nucleic acid labeling kits.*

Label IT Nucleic Acid Labeling Reagents were prepared prior to first time use according to the manufacturer's protocol. In a 200 µL PCR tube, a 50 µL reaction was prepared by adding 35 µL DNase-, RNase-free (molecular biology-grade water + 5 µL 10X Labeling Buffer A + 5 µL 1 mg/mL nucleic acid sample (sgRNA) + 5 µL *Label* IT

Reagent, in that order. The reaction was incubated in a thermocycler for 1 hour at 37°C and briefly centrifuged halfway through to minimize evaporation.

The alternative method for purification, using ethanol precipitation opposed to G50 microspin column, was used because quantification of the sgRNA was necessary. Nucleic acids purified by the microspin column can lead to erroneously high ultraviolet A260 readings. The labeling reaction was brought up to 100 µL with molecular biology-grade water, then 0.1 volumes of 5M NaCl and 2-2.5 volumes of ice cold 100% ethanol were added to the reaction and mixed well, then placed at -20°C for at least 30 minutes. Tube orientation was marked, and the labeled sgRNA was pelleted by centrifugation at 17,000g and 4°C for 30 minutes. All ethanol was gently removed by pipetting, the pellet was washed with 500 µL room temperature 70% ethanol, and the tube was centrifuged with the prior conditions. All ethanol was gently removed, and the pellet did not dry more than 5 minutes. The fluorescein labeled sgRNA pellet was resuspended in 50 µL of sterile water and quantified by nanodrop. Purified labeled sgRNA was stored on ice for immediate use or at -20°C for long-term storage.

The 1:1 (v:w) ratio of *Label* IT Reagent to nucleic acid described here typically results in a labeling density of one label per every 20-60 bases. Calculating the base:dye ratio may be done by measuring the absorbance of your labeled sample at 260 nm (A_{260}) and at lambda max (A_{dye}). $\boldsymbol{\lambda}_{max}$ for fluorescein is 494 nm. Since the *Label* IT dye may contribute to the absorbance at 260 nm, a correction may be calculated using A_{base}. The correction factor ($C.F._{260}$) value for fluorescein is 0.32. The extinction coefficient for nucleic acid bound fluorescein dye ($\boldsymbol{\varepsilon_{dye}}$) is 68,000, and the extinction coefficient of

nucleic acid ($\boldsymbol{\varepsilon_{base}}$)for RNA is 8,250. Equations 1-3 are used to calculate the base:dye ratio.

$$\boldsymbol{A_{base} = A_{260} - (A_{dye} * C.F._{\cdot 260})} \quad (1)$$

$$\boldsymbol{C.F._{\cdot 260} = A_{260}\ \text{free dye} / A_{\lambda max}\ \text{free dye}} \quad (2)$$

$$\boldsymbol{\text{base: dye} = (A_{base} * \varepsilon_{dye}) / (A_{dye} * \varepsilon_{base})} \quad (3)$$

3. Antibody-conjugated Graphene Oxide (Ab-GO)

Antibody conjugated GO was synthesized by a classic two-step EDC-NHS (1-Ethyl-3 -(3- dimethylaminopropyl) carbodiimide and N-hydroxysuccinimide) method. A 1 mL mixture of 20 µg/mL GO in 5mM MES pH 4.0 was prepared and sonicated for 10 minutes. A 1 mL mixture of 4 mg/mL EDC + 6mg/mL NHS was prepared and added to the sonicated mixture to activate the GO. The reaction was stirred for 15 minutes at 15°C followed by centrifugation at 29,000g for 10 minutes. The EDC+NHS activated GO pellet was resuspended in 1 µL of 1mg/mL dCas9 antibody + 99 µL of 20 mM PBS pH 7.4 to modify the GO with the antibody. The reaction was shaken for 2 hours at 15°C. Then, 100 µL of 2% BSA in 20 mM PBS pH 7.4 was added for blocking the remaining active sites of GO for 30 minutes. Unbound dCas9 antibody was removed by centrifuging at 29,000g for 20 minutes. The supernatant was discarded, and the pellet was resuspended in 100 µL PBS pH 7.4, vortexed thoroughly and stored at 4°C.

Atomic force microscopy (AFM) was used to characterize the height profiles of bare GO, the EDC: NHS activated GO, and the Ab-GO. Sample solutions of bare GO or modified GO were dripped on freshly cleaved glass surface using a pipette and then dried in ambient air. Surface topographic features were scanned in contact mode using a commercial AFM (CSPM4000, Benyuan, China) equipped with a silicon cantilever.

4. Quenching Efficiency Assay

The quenching efficiency assay confirms the optimal Ab-GO concentration for use in this system by determining the concentration with the lowest quenching efficiency percentage. It is expected that oversaturation of Ab-GO would cause significant errors as the density of soluble Ab-GO would be so high that the dissociation of dCas9/sgRNA and Ab-GO would not generate enough space between the labeled sgRNA and the Ab-GO surface. Thus, excess Ab-GO would be unfavorable for desorption of dCas9/sgRNA from the Ab-GO surface. Using the minimal amount of Ab-GO for the assay would differentiate signals from varying DNA concentrations. Quenching efficiency percentages were calculated for each Ab-GO concentration in the assay.

The SPECTRA max 190 Microplate Spectrophotometer was used for incubation, and the Biotek Synergy H1 microplate reader (Gen5 software) was used to measure the florescence emission spectrum from 400 to 700 nm. The final concentrations of each component were 15.82 nM dCas9, 1.166 nM labeled-sgRNA, 10 nM genomic DNA, and an Ab-GO concentration in the range of 0, 2, 3, and 5 μg/mL. Each component was typically added the reaction using 20 μL of 10X of the final concentration, and the total volume for each well was brought up to 200 μL using duplex buffer.

To wells in a clean corning 96-well black plate, duplex buffer was added, followed by a 20 µL of 10X concentration of Ab-GO and then 500 ng dCas9, in that order. The reaction was incubated for 30 min at 37 °C. At the end of the first incubation, 100 ng of labeled-sgRNA was added to the dCas9/Ab-GO complex and incubated again for 30 min at 37 °C to form the ribonucleoprotein duplex on the GO platform. Lastly, 20 µL of 10X concentration of genomic target DNA was added and incubated for 20 min at 37 °C.

Optical measurements were performed under ambient conditions at room temperature. Data was collected in duplicate, and the average fluorescence intensity and standard deviation were calculated. A Stern−Volmer plot was made of F_0/F against the concentration of Ab-GO, where F_0 and F were the fluorescence intensity at the maxima in the absence and presence of Ab-GO, respectively. The quenching efficiency of fluorescein labeled sgRNAs by AB-GO was calculated using equation 4, where F_0 and F are the fluorescence intensity at the maxima in the absence and presence of Ab-GO, respectively.

$$\% \textbf{ Quenching efficiency} = 100 - \frac{F}{F_0} x\ 100\% \quad (4)$$

CHAPTER III - RESULTS AND DISCUSISON

1. Protein Purification

After purification of dCas9 on the nickel column, SDS-PAGE gel analysis confirmed the presence of the dCas9 fusion protein (202.4 kDa, red arrow). The 6His-MBP fusion tag (41.2 kDa, gray arrow) was cleaved from dCas9 (158.3 kDa, green arrow) by TEV protease, and the cleavage fragments were confirmed by SDS-PAGE gel as seen in Figure 10.

dCas9-TEV-MBP-6His	**202.4 kDa**
dCas9	**158.3 kDa**
MBP	**40.2 kDa**
6xHis	**840.9 Da**
TEV cleavage site	**869.9 Da**
6xHis-MBP	**41.2 kDa**

Table 1: Expected protein sizes.

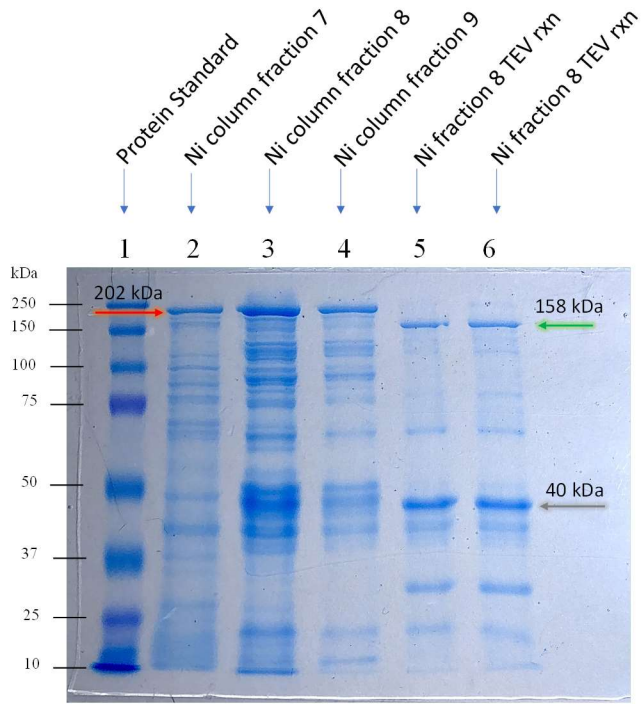

Figure 10: Nickel column and TEV cleavage SDS-PAGE analysis.

Purification of His-tagged Proteins by Batch Method

On the SDS-PAGE gel in Figure 10, fractions 1-7 are check points of purification using the His-Pur Ni-NTA resin. This method purified his-tagged proteins due to high affinity of histidine to the Ni resin. After washing steps to remove unbound and weakly bound proteins, a high imidazole buffer was used to elute the his-tagged proteins. Imidazole has higher affinity for Ni-NTA resin and displaces the his-tagged proteins. We are interested in purifying dCas9, which should be recovered in the flowthrough or wash steps. Fraction 2 is the flowthrough and has no visible bands. The flowthrough was concentrated using a 100 kDa filter. Faction 3 is the concentrated flowthrough sample, and fraction 2 is the flowthrough of fraction 3. Both fractions 2 and 3 have no visible bands, indicating dCas9 was not purified during this step. Fractions 4 and 5 are collected after wash steps with buffer containing 10 and 25 mM imidazole, respectively. Fraction 4

has one visible protein band at 158 kDa, which indicated that dCas9 has been purified using the Ni-NTA resin. This result also implies that dCas9 binds weakly to the resin. Fraction 5 does not have a clear band, but dCas9 is still visible after elution with a high imidazole concentration of 250 mM, as seen in fraction 7. Purifying dCas9 using this method is possible, as seen in fraction 5, but the wash steps may need to be optimized with a slightly higher imidazole concentration to have a higher dCas9 yield, with less dCas9 remaining in the eluate. In fraction 7, the eluate has a few faint bands and a strong band at 41 kDa which is the 6his-MBP tag.

Cation Exchange

The isoelectric point (pI) of dCas9 is 9.01 as determined by the amino acid sequence (using ExPASy online tool: https://web.expasy.org/compute_pi/). On cation resin, dCas9 carries a positive charge (in the appropriate pH buffer) and binds the negatively charged resin. The proteins were eluted in an order depending on their net surface charge using a linear gradient of buffer B containing 100 mM – 500 mM KCl. Fractions loaded on this SDS-PAGE gel were concentrated using a 100 kDa filter. Fractions 7-8 in Figure 11 are the concentrated eluted fractions of 300 mM, 400 mM, and 500 mM KCl buffers, respectively. Fraction 10 has one visible protein band at 158 kDa, which indicates that dCas9 has been purified by cation exchange. Fraction 9 is similar to fraction 10, but the dCas9 band is fainter. After TEV cleavage, cation exchange chromatography proved to yield pure dCas9.

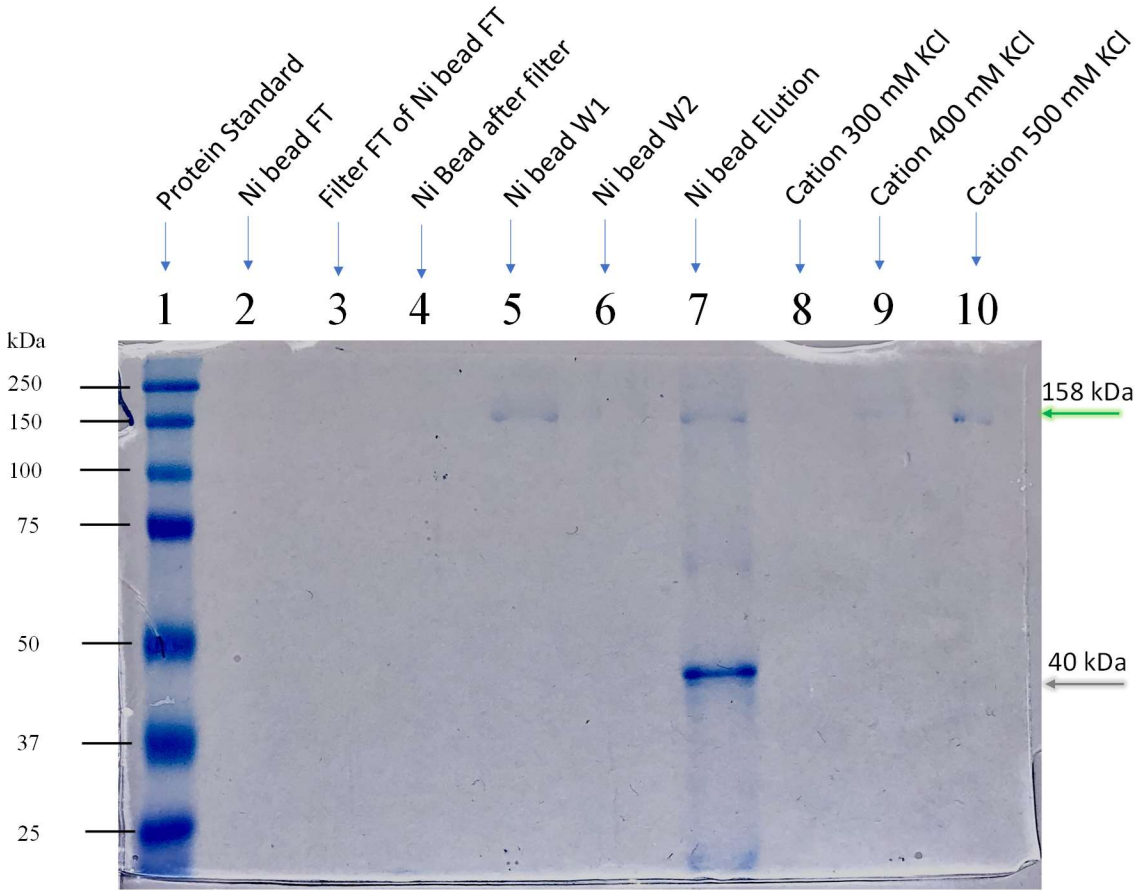

Figure 11: Ni-NTA resin and cation exchange chromatography SDS-PAGE analysis.

2. sgRNA Template Synthesis

In our prior work, six sgRNAs candidates were designed to target sequences on the tetM gene. In this work, with the goal of determining the optimal Ab-GO concentration for use in assay, only one sgRNA template was synthesized for use in the quenching efficiency assay. According to the Guide-it invitro transcription kit protocol, a 130 bp band is expected for confirmation of sgRNA template synthesis, and this is confirmed in Figure 12. The sgRNA was synthesized from the synthesized sgRNA DNA template by the invitro transcription reaction.

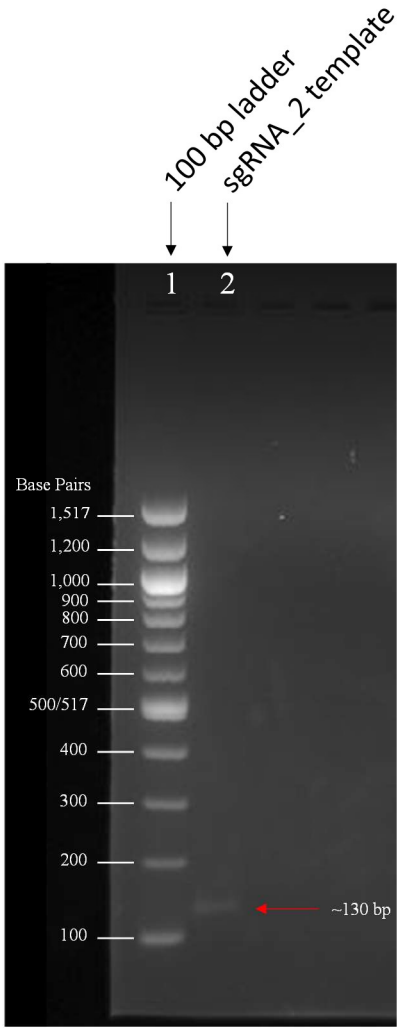

Figure 12: sgRNA_2 DNA template synthesis.

2.1 Cas9 Cleavage Assay Before sgRNA Labeling

Target T2 on the tetM gene was used in the quenching efficiency assay, thus sgRNA_2 was synthesized from its corresponding template. To confirm the successful synthesis of a functioning sgRNA_2, the cleavage assay was performed. The PCR amplified T2 target DNA is 630 bp, and it was successfully cleaved in the assay into two unequal fragments at 370 and 260 bp as seen in lanes 3 and 4 in Figure 13. Lane 2 contains the uncut T2 DNA as a control. The following experiment is sgRNA labeling.

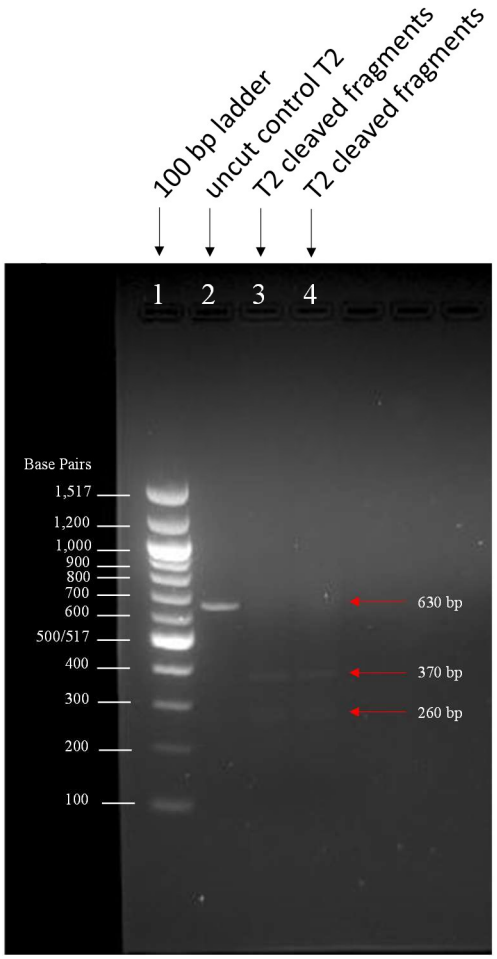

Figure 13: Cas9 cleavage assay before sgRNA labeling.

2.2 Cas9 Cleavage Assay After sgRNA Labeling

After labeling sgRNA_2 with fluorescein, the labeled sgRNA should be screened by cleavage assay again to ensure that the binding specificity is retained. Again, amplified T2 target DNA is 630 bp, and it was successfully cleaved in the assay into two unequal fragments at 370 and 260 bp as seen in lanes 3 in Figure 14. Lane 2 contains the uncut T2 DNA as a control.

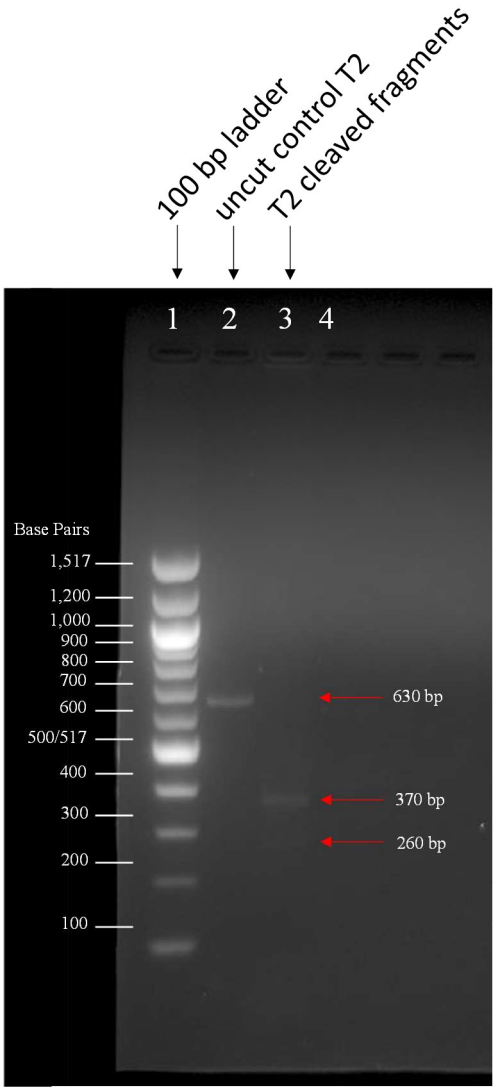

Figure 14: Cas9 cleavage assay after sgRNA labeling.

Sample ID	base:dye ratio
sgRNA_2 #0	52.99
sgRNA_2 #1	50.94
sgRNA_2 #2	52.26
sgRNA_2 #3	63.3
sgRNA_2 #4	48.88

Table 2: base:dye labeling ratios for sgRNA_2.

After confirming labeled sgRNA_2 was functional, equations 1-3 were used to calculate the labeling ratios for each prepared batch. For example, a ratio of 50 would

indicate one label per every 50 bases. The length of sgRNA_2 is ~130 bp, so on average two fluorescein molecules are covalently labeled to the sgRNA.

3. Ab-GO Surface Morphologies

Atomic force microscopy (AFM) was introduced to characterize the GO surface modifications. According to Huang et al., the height of GO would obviously increase after being activated by EDC-NHS and further upon conjugation by antibodies.[23] This study served as a reference point for us to use AFM to characterize the surface morphologies of bare GO, EDC-NHS-activated GO, and antibody-conjugated GO (Ab-GO) to provide evidence of the EDC-NHS coupling reaction and the presence of antibodies on the GO surface. In Figure 15(A), bare GO has a thin and flat appearance with a height of approximately 1 nm on the glass slide, which corresponds to the monolayer state of GO. The corresponding line scan and height profile of the sample is shown in Figure 15(B). After activation by EDC-NHS, GO exhibited an increased thickness of approximately 7 nm. The line scan gave a corresponding cross-sectional height profile in Figure 16 (B), showing a uniform surface of the GO. Compared to GO, the 150 kDa Cas9 antibody is very large. The antibody-conjugated GO should reflect this in the AFM characterization. As shown in Figure 17 (A), the height of Ab-GO increased dramatically, with a typical thickness of about 12 nm, as suggested in the height profile in Figure 17 (B). Some bright peaks were observed on this sample, which was also similar to the report of our reference, and they are likely a result of the accumulation of antibodies on the GO surface. All of the surface morphology results implied that the antibody was successfully conjugated on the GO surface.

(A) (B)

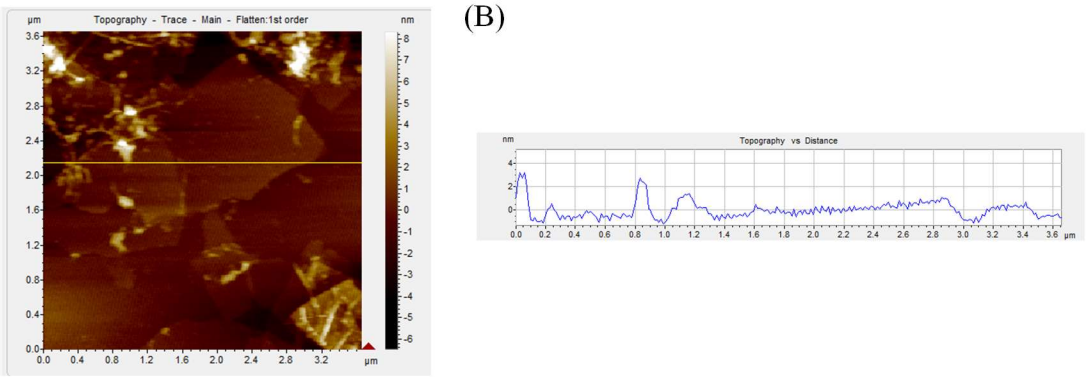

Figure 15: Bare GO AFM surface morphology (A) and height profile (B).

(A) (B)

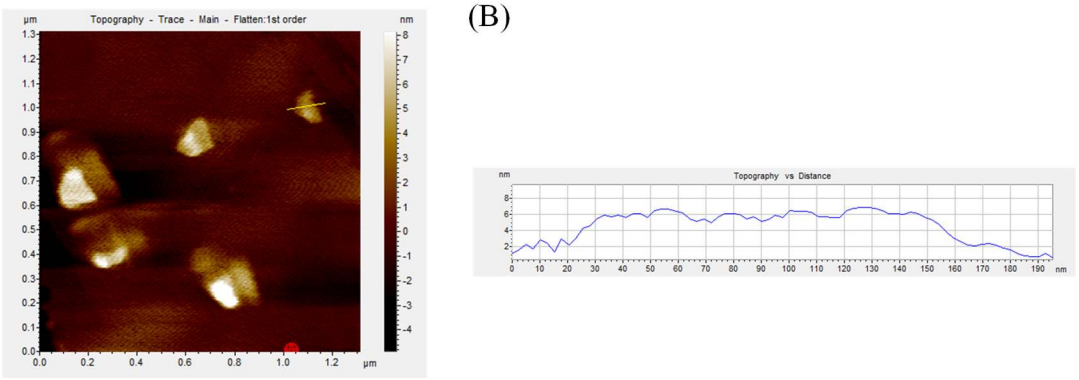

Figure 16: GO activated with EDC: NHS AFM surface morphology (A) and height profile (B).

(A) (B)

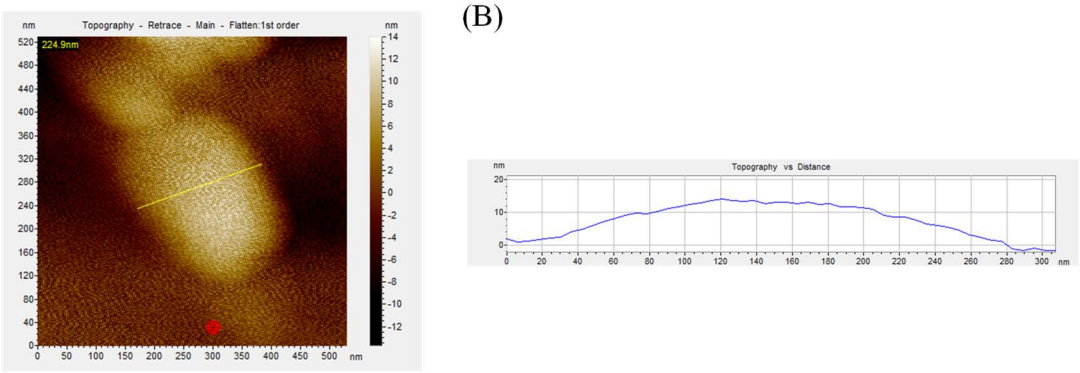

Figure 17: Ab-GO AFM surface morphology (A) and height profile (B).

4. Quenching Efficiency Assay

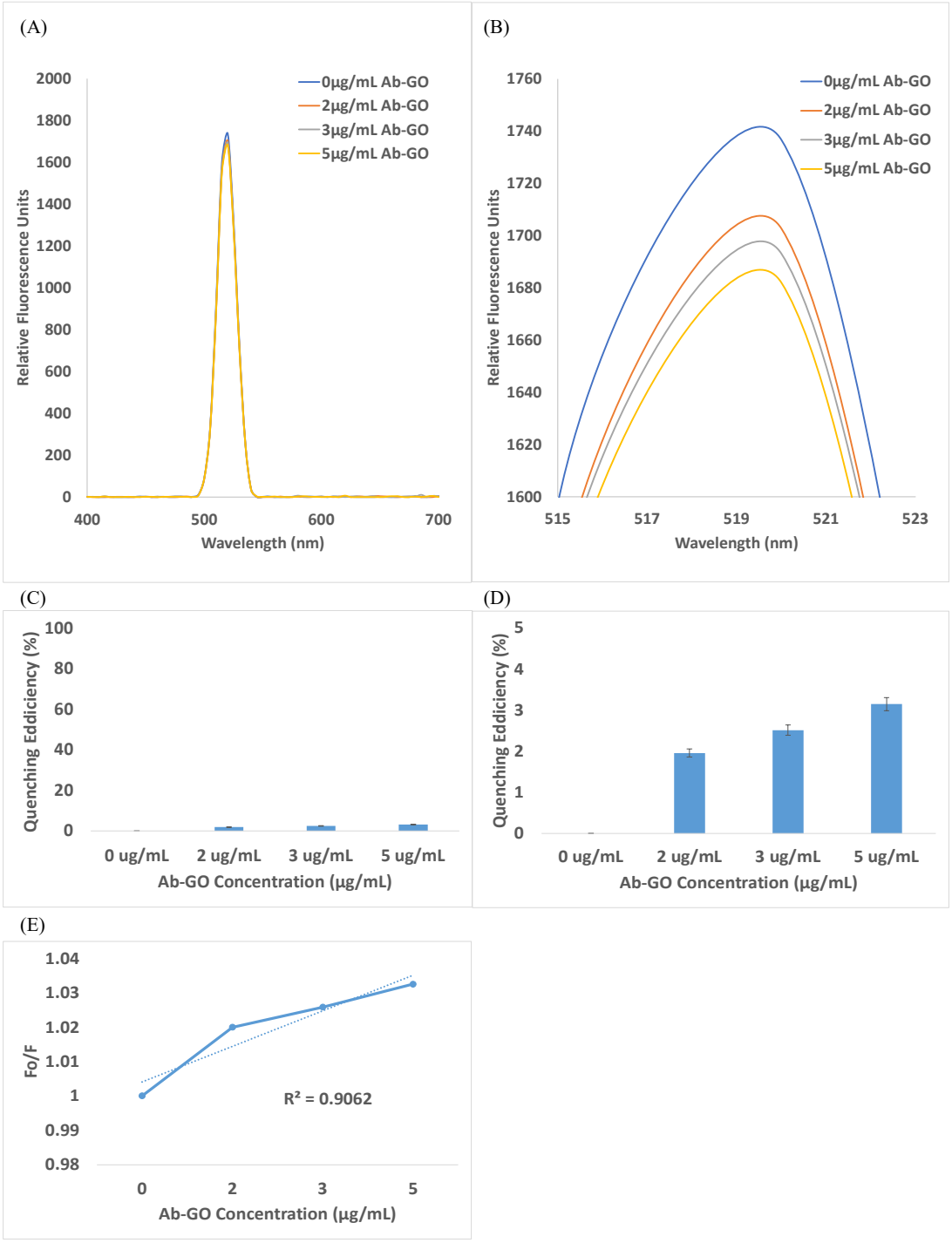

Figure 18: Quenching efficiency analysis. Assay plot from 400 – 700 nm (A) and zoomed in (B). Quenching efficiency % bar chart scaled to 100% (C) and zoomed in to a 5% scale (D). Stern-volmer plot (E).

The effect of Ab-GO concentrations on the quenching of labeled sgRNA was studied over the range from 0 to 5 μg/mL. The quenching efficiency increased with increasing concentrations of Ab-GO (Figure 18A,B). Further analysis on quenching efficiency percentage was performed to determine the lowest GO concentration for the assay (Figure 18C,D). At 2 μg/mL of Ab-GO, the quenching efficiency was calculated to be ~2%. When the GO concentration was less than 2 μg/mL, there was a minimal quenching effect of labeled sgRNA, which could be due to the incomplete adsorption of dCas9 on the Ab-GO surface. Thus, 2 μg/mL of GO was determined to be the optimal Ab-GO concentration for use in this system. A stern-volmer plot was made (Figure 18E), but the anticipated linear quenching correlated to Ab-GO concentration cannot be statistically assumed outside of the tested concentration range. Increasing the Ab-GO concentration range would be sufficient for mathematically describing the Ab-GO impact on quenching, but it is not necessary for choosing the optimal Ab-GO concentration for the assay.

A point of discussion for this assay is the potential for some labeled sgRNAs themselves to adsorb on a bare GO surface through $\boldsymbol{\pi}$-$\boldsymbol{\pi}$ stacking. Single stranded DNA (ssDNA), or sgRNA in this case, preferentially interact with GO compared to dsDNA. Notably, the GO surface used in this system is not bare since it is conjugated with antibodies and blocked with BSA. The unwanted potential adsorption of sgRNA to bare GO is less likely to occur when using Ab-GO since less of the GO surface is available for interaction with sgRNA. Additionally, if some sgRNA would adsorb to bare GO on the Ab-GO surface, it is unlikely to affect the fluorescence recovery signal generated upon

DNA detection since sgRNA has a relatively strong affinity to GO and will be quenched unless it is desorbed.

Interestingly, mechanisms of desorption of preadsorbed fluorescent ssDNA (f-ssDNA) from GO, driven by the addition of complementary DNA (cDNA) and non-cDNA, were studied.[21] Desorption of f-ssDNA from GO was indicated by an increase in fluorescence signal. Single stranded cDNAs and non-cDNAs were used to assess desorption mechanisms of f-ssDNA from GO. Additionally, partial dsDNA (pdsDNA) with either c-ssDNA or non-c-ssDNA tails were assessed to promote desorption since a portion of the probe is partially dsDNA, which has lower affinity to GO. At low GO concentrations less than 10 μg/mL, f-ssDNAs were desorbed from the GO following both hybridization with cDNA on the GO surface or via nonspecific simple displacement by non-cDNA due to the law of mass action. At 10 μg/mL GO, the incoming DNAs themselves were more likely to adsorb onto the GO rather than hybridize with or displace the f-ssDNA. This is of interest to consider since a portion of the tetM target dsDNA is indeed complementary to a portion of the sgRNA. However, this study discussing the mechanisms of DNA desorption from GO highlighted that the key for f-ssDNA desorption from GO with any of the cDNA (c-ssDNA or c-pdsDNA) is the hybridization between the adsorbed f-ssDNA and incoming ssDNA complements. Our dsDNA targets would not desorb sgRNA since they may not directly hybridize, and our targets would not likely displace adsorbed sgRNA on GO since dsDNAs have a lower affinity toward GO.

CHAPTER 4 - CONCLUSIONS

A new dCas9 protein purification protocol was established in our lab, and the quenching assay was performed as per the aims of the study. First, dCas9 expressed from pMJ841 was purified, yet the purification protocols were not fully optimized for producing a high yield. Second, the preliminary results of the quenching efficiency assay data suggest that 2 μg/mL is the optimal concentration for use in this assay since it is the minimal concentration. A broader range of Ab-GO concentrations was not yet fully assessed on the stern-volmer plot to mathematically describe the quenching function.

For the quenching efficiency assay, using fluorescein as the fluorescent probe for sgRNA labeling was an important change compared to Alexa-488 used in our prior work. Alexa-488 previously caused an "overflow" reading during spectral scanning in the quenching efficiency assay. The overflow was avoided in the quenching efficiency assay with fluorescein in this work to determine to optimal Ab-GO concentration in the assay.

We are currently adjusting the protein purification protocol for a higher yield of pure dCas9. Then, we will continue with multiplexed detection of different pathogenic dsDNAs by using different sgRNAs and fluorophore labels. Further, we aim to detect cell lysates of ARBs to characterize our system for use as a DNA diagnostic technology for combating antibiotic resistance.

BIBLIOGRAPHY

1. Quan, J.; Langelier, C.; Kuchta, A.; Batson, J.; Teyssier, N.; Lyden, A.; Caldera, S.; McGeever, A.; Dimitrov, B.; King, R.; Wilheim, J.; Murphy, M.; Ares, L. P.; Travisano, K. A.; Sit, R.; Amato, R.; Mumbengegwi, D. R.; Smith, J. L.; Bennett, A.; Gosling, R.; Mourani, P. M.; Calfee, C. S.; Neff, N. F.; Chow, E. D.; Kim, P. S.; Greenhouse, B.; DeRisi, J. L.; Crawford, E. D., FLASH: a next-generation CRISPR diagnostic for multiplexed detection of antimicrobial resistance sequences. *Nucleic Acids Res* **2019,** *47* (14), e83.

2. Lerminiaux, N. A.; Cameron, A. D. S., Horizontal transfer of antibiotic resistance genes in clinical environments. *Can J Microbiol* **2019,** *65* (1), 34-44.

3. Golkar, Z.; Bagasra, O.; Pace, D. G., Bacteriophage therapy: a potential solution for the antibiotic resistance crisis. *J Infect Dev Ctries* **2014,** *8* (2), 129-36.

4. Davies, J.; Davies, D., Origins and evolution of antibiotic resistance. *Microbiol Mol Biol Rev* **2010,** *74* (3), 417-33.

5. Ha, D. T.; Nguyen, V. T.; Kim, M. S., Graphene Oxide-Based Simple and Rapid Detection of Antibiotic Resistance Gene via Quantum Dot-Labeled Zinc Finger Proteins. *Anal Chem* **2021,** *93* (24), 8459-8466.

6. Gootenberg, J. S.; Abudayyeh, O. O.; Kellner, M. J.; Joung, J.; Collins, J. J.; Zhang, F., Multiplexed and portable nucleic acid detection platform with Cas13, Cas12a, and Csm6. *Science* **2018,** *360* (6387), 439-444.

7. Myhrvold, C.; Freije, C. A.; Gootenberg, J. S.; Abudayyeh, O. O.; Metsky, H. C.; Durbin, A. F.; Kellner, M. J.; Tan, A. L.; Paul, L. M.; Parham, L. A.; Garcia, K.

F.; Barnes, K. G.; Chak, B.; Mondini, A.; Nogueira, M. L.; Isern, S.; Michael, S. F.; Lorenzana, I.; Yozwiak, N. L.; MacInnis, B. L.; Bosch, I.; Gehrke, L.; Zhang, F.; Sabeti, P. C., Field-deployable viral diagnostics using CRISPR-Cas13. *Science* **2018,** *360* (6387), 444-448.

8. Ha, D. T.; Ghosh, S.; Ahn, C. H.; Segal, D. J.; Kim, M. S., Pathogen-specific DNA sensing with engineered zinc finger proteins immobilized on a polymer chip. *Analyst* **2018,** *143* (17), 4009-4016.

9. Zhang, Y.; Qian, L.; Wei, W.; Wang, Y.; Wang, B.; Lin, P.; Liu, W.; Xu, L.; Li, X.; Liu, D.; Cheng, S.; Li, J.; Ye, Y.; Li, H.; Zhang, X.; Dong, Y.; Zhao, X.; Liu, C.; Zhang, H. M.; Ouyang, Q.; Lou, C., Paired Design of dCas9 as a Systematic Platform for the Detection of Featured Nucleic Acid Sequences in Pathogenic Strains. *ACS Synth Biol* **2017,** *6* (2), 211-216.

10. Zhou, W.; Hu, L.; Ying, L.; Zhao, Z.; Chu, P. K.; Yu, X. F., A CRISPR-Cas9-triggered strand displacement amplification method for ultrasensitive DNA detection. *Nat Commun* **2018,** *9* (1), 5012.

11. Huang, M.; Zhou, X.; Wang, H.; Xing, D., Clustered Regularly Interspaced Short Palindromic Repeats/Cas9 Triggered Isothermal Amplification for Site-Specific Nucleic Acid Detection. *Anal Chem* **2018,** *90* (3), 2193-2200.

12. Makarova, K. S.; Wolf, Y. I.; Alkhnbashi, O. S.; Costa, F.; Shah, S. A.; Saunders, S. J.; Barrangou, R.; Brouns, S. J.; Charpentier, E.; Haft, D. H.; Horvath, P.; Moineau, S.; Mojica, F. J.; Terns, R. M.; Terns, M. P.; White, M. F.; Yakunin, A. F.; Garrett, R. A.; van der Oost, J.; Backofen, R.; Koonin, E. V., An updated evolutionary classification of CRISPR-Cas systems. *Nat Rev Microbiol* **2015,** *13* (11), 722-36.

13. Hryhorowicz, M.; Lipiński, D.; Zeyland, J.; Słomski, R., CRISPR/Cas9 Immune System as a Tool for Genome Engineering. *Arch Immunol Ther Exp (Warsz)* **2017,** *65* (3), 233-240.

14. Zhou, L.; Peng, R.; Zhang, R.; Li, J., The applications of CRISPR/Cas system in molecular detection. *J Cell Mol Med* **2018,** *22* (12), 5807-5815.

15. Koo, B.; Kim, D. E.; Kweon, J.; Jin, C. E.; Kim, S. H.; Kim, Y.; Shin, Y., CRISPR/dCas9-mediated biosensor for detection of tick-borne diseases. *Sens Actuators B Chem* **2018,** *273*, 316-321.

16. Guk, K.; Keem, J. O.; Hwang, S. G.; Kim, H.; Kang, T.; Lim, E. K.; Jung, J., A facile, rapid and sensitive detection of MRSA using a CRISPR-mediated DNA FISH method, antibody-like dCas9/sgRNA complex. *Biosens Bioelectron* **2017,** *95*, 67-71.

17. Nishimasu, H.; Cong, L.; Yan, W. X.; Ran, F. A.; Zetsche, B.; Li, Y.; Kurabayashi, A.; Ishitani, R.; Zhang, F.; Nureki, O., Crystal Structure of Staphylococcus aureus Cas9. *Cell* **2015,** *162* (5), 1113-26.

18. Chen, W.; Zhang, H.; Zhang, Y.; Wang, Y.; Gan, J.; Ji, Q., Molecular basis for the PAM expansion and fidelity enhancement of an evolved Cas9 nuclease. *PLoS Biol* **2019,** *17* (10), e3000496.

19. Li, S.; Mulloor, J. J.; Wang, L.; Ji, Y.; Mulloor, C. J.; Micic, M.; Orbulescu, J.; Leblanc, R. M., Strong and selective adsorption of lysozyme on graphene oxide. *ACS Appl Mater Interfaces* **2014,** *6* (8), 5704-12.

20. Li, S.; Aphale, A. N.; Macwan, I. G.; Patra, P. K.; Gonzalez, W. G.; Miksovska, J.; Leblanc, R. M., Graphene oxide as a quencher for fluorescent assay of amino acids, peptides, and proteins. *ACS Appl Mater Interfaces* **2012,** *4* (12), 7069-75.

21. Park, J. S.; Goo, N. I.; Kim, D. E., Mechanism of DNA adsorption and desorption on graphene oxide. *Langmuir* **2014,** *30* (42), 12587-95.

22. Chang, H.; Tang, L.; Wang, Y.; Jiang, J.; Li, J., Graphene fluorescence resonance energy transfer aptasensor for the thrombin detection. *Anal Chem* **2010,** *82* (6), 2341-6.

23. Huang, A.; Li, W.; Shi, S.; Yao, T., Quantitative Fluorescence Quenching on Antibody-conjugated Graphene Oxide as a Platform for Protein Sensing. *Sci Rep* **2017,** *7*, 40772.

24. Hajian, R.; Balderston, S.; Tran, T.; deBoer, T.; Etienne, J.; Sandhu, M.; Wauford, N. A.; Chung, J. Y.; Nokes, J.; Athaiya, M.; Paredes, J.; Peytavi, R.; Goldsmith, B.; Murthy, N.; Conboy, I. M.; Aran, K., Detection of unamplified target genes via CRISPR-Cas9 immobilized on a graphene field-effect transistor. *Nat Biomed Eng* **2019,** *3* (6), 427-437.

25. Chua, C. K.; Pumera, M., The reduction of graphene oxide with hydrazine: elucidating its reductive capability based on a reaction-model approach. *Chem Commun (Camb)* **2016,** *52* (1), 72-5.

26. Zhang, X.; Hu, Y.; Yang, X.; Tang, Y.; Han, S.; Kang, A.; Deng, H.; Chi, Y.; Zhu, D.; Lu, Y., FÖrster resonance energy transfer (FRET)-based biosensors for biological applications. *Biosens Bioelectron* **2019,** *138*, 111314.

27. Mardenborough, Y. S. N.; Nitsenko, K.; Laffeber, C.; Duboc, C.; Sahin, E.; Quessada-Vial, A.; Winterwerp, H. H. K.; Sixma, T. K.; Kanaar, R.; Friedhoff, P.; Strick, T. R.; Lebbink, J. H. G., The unstructured linker arms of MutL enable GATC site

incision beyond roadblocks during initiation of DNA mismatch repair. *Nucleic Acids Res* **2019,** *47* (22), 11667-11680.

28. Jinek, M.; Chylinski, K.; Fonfara, I.; Hauer, M.; Doudna, J. A.; Charpentier, E., A programmable dual-RNA-guided DNA endonuclease in adaptive bacterial immunity. *Science* **2012,** *337* (6096), 816-21.